



# SARS-CoV-2 and Influenza A Virus Coinfections in Ferrets

Ying Huang,<sup>a</sup> Amanda L. Skarlpka,<sup>a</sup> Hyesun Jang,<sup>a</sup> Uriel Blas-Machado,<sup>b</sup> Nathan Holladay,<sup>c</sup> R. Jeffrey Hogan,<sup>a,c,d</sup>  Ted M. Ross<sup>a,c</sup>

<sup>a</sup>Center for Vaccines and Immunology, University of Georgia, Athens, GA, USA

<sup>b</sup>Department of Pathology, University of Georgia, Athens, GA, USA

<sup>c</sup>Department of Infectious Diseases, University of Georgia, Athens, GA, USA

<sup>d</sup>Veterinary Biosciences and Diagnostic Imaging, University of Georgia, Athens, GA, USA

**ABSTRACT** Severe acute respiratory syndrome coronavirus 2 (SARS-CoV-2) and seasonal influenza viruses are cocirculating in the human population. However, only a few cases of viral coinfection with these two viruses have been documented in humans with some people having severe disease and others mild disease. To examine this phenomenon, ferrets were coinfecting with SARS-CoV-2 and human seasonal influenza A viruses (IAVs; H1N1 or H3N2) and were compared to animals that received each virus alone. Ferrets were either immunologically naive to both viruses or vaccinated with the 2019 to 2020 split-inactivated influenza virus vaccine. Coinfected naive ferrets lost significantly more body weight than ferrets infected with each virus alone and had more severe inflammation in both the nose and lungs compared to that of ferrets that were single infected with each virus. Coinfected, naive animals had predominantly higher IAV titers than SARS-CoV-2 titers, and IAVs were efficiently transmitted by direct contact to the cohoused ferrets. Comparatively, SARS-CoV-2 failed to transmit to the ferrets that cohoused with coinfecting ferrets by direct contact. Moreover, vaccination significantly reduced IAV titers and shortened the viral shedding but did not completely block direct contact transmission of the influenza virus. Notably, vaccination significantly ameliorated influenza-associated disease by protecting vaccinated animals from severe morbidity after IAV single infection or IAV and SARS-CoV-2 coinfection, suggesting that seasonal influenza virus vaccination is pivotal to prevent severe disease induced by IAV and SARS-CoV-2 coinfection during the COVID-19 pandemic.

**IMPORTANCE** Influenza A viruses cause severe morbidity and mortality during each influenza virus season. The emergence of SARS-CoV-2 infection in the human population offers the opportunity to potential coinfections of both viruses. The development of useful animal models to assess the pathogenesis, transmission, and viral evolution of these viruses as they coinfect a host is of critical importance for the development of vaccines and therapeutics. The ability to prevent the most severe effects of viral coinfections can be studied using effect coinfection ferret models described in this report.

**KEYWORDS** SARS-CoV-2, influenza, coinfection, ferrets, vaccination, disease severity, viral transmission

The coronavirus disease 2019 (COVID-19) pandemic has resulted in over 233 million infections and ~4.77 million deaths worldwide (<http://covid19.who.int/>). This disease is caused by the severe acute respiratory syndrome coronavirus-2 (SARS-CoV-2) virus that emerged in China in 2019 (1). Infected people have a range of clinical outcomes from asymptomatic to severe disease and death (2). Currently, SARS-CoV-2 cases are still surging in the United States, and the continuously mutating virus is spreading easily among the population (3–8). Although the USA government has implemented COVID-19 vaccine programs since December 2020, only 56% of the

**Editor** Colin R. Parrish, Cornell University

**Copyright** © 2022 American Society for Microbiology. All Rights Reserved.

Address correspondence to Ted M. Ross, tedross@uga.edu.

The authors declare no conflict of interest.

**Received** 19 October 2021

**Accepted** 16 December 2021

**Accepted manuscript posted online**

22 December 2021

**Published** 9 March 2022

population had been fully vaccinated as of October 2021 (<http://ourworldindata.org/>). This level is still far below the percentage for herd immunity. Moreover, SARS-CoV-2 antibody levels started to decline 6 months postvaccination (9). Thus, people who have not been vaccinated or have been vaccinated longer than 6 months remain in danger of potential infection or reinfection (10, 11).

As SARS-CoV-2 infections continue, the Northern hemisphere is approaching the 2021 to 2022 influenza season. In general, it is difficult to predict the severity of an influenza season and which subtypes of influenza virus will dominate at various points during the season. Social distancing and mask-wearing may affect the transmission and spread of influenza viruses because influenza cases were severely reduced during the 2020 influenza season in the Southern hemisphere (12). These countermeasures also have some effect on influenza virus transmission for people living in the Northern hemisphere, but there will be regional differences based upon the implementation of these practices and local lockdown restrictions.

Since the outbreak of COVID-19 at the end of 2019, the WHO had launched a global campaign to test therapeutic agents and vaccines on an unprecedented scale (13–15). During this progress, several animal models, including angiotensin-converting enzyme 2 (ACE2) transgenic mice, Syrian hamsters, ferrets, and nonhuman primates, were established to investigate the virus pathogenicity and facilitate preclinical analysis for vaccines and therapeutics (16, 17). Due to the accessibility and cost efficiency, mice, hamsters, and ferrets were more commonly used for preclinical screening. However, no ideal animal model could mimic SARS-CoV-2 infection in humans, and each animal model has its advantages and limitations. The transgenic mouse model expresses the human ACE2 gene, enabling the SARS-CoV-2 virus to bind and enter cells and initiate viral infection. Those mice express human ACE2 under different promoters, which results in a range of mild to lethal diseases, and mice can develop encephalitis after infection with SARS-CoV-2 (18–20). The limitation of ACE2 transgenic mice is that the human ACE2 gene is expressed ectopically, which may change the tissue or cellular tropism of the virus (21). The Syrian hamster is a promising animal model to investigate virus pathogenicity and access vaccines and therapeutics (17, 22). Although SARS-CoV-2 infection was not lethal in hamsters, infected animals showed mild-to-moderate disease with progressive body weight loss that began 1 to 2 d postinfection (pi) along with clinical morbidity, including lethargy, ruffled fur, a hunched posture, and labored breathing (23). The virus was detectable in both upper and lower respiratory tracts (24). However, ferrets are a gold-standard model for accessing the pathogenicity and transmission of human respiratory viruses (25), including influenza virus and respiratory syncytial virus. When experimentally infected with SARS-CoV-2, there are no observed clinical symptoms, and body weight alternation was observed postinfection, but virus shedding was observed in nasal swabs (26–28).

Both influenza and COVID-19 are contagious respiratory illnesses caused by the infection of two different pathogens: influenza virus (IAV) and SARS-CoV-2 virus. Influenza and COVID-19 present many similar symptoms, such as fever, cough, headache, sore throat, and pneumonia, and acute respiratory distress syndrome (29, 30), which makes it difficult for medical professionals to diagnose and provide a course of action. Moreover, IAV and SARS-CoV-2 are both airborne transmitted viruses that infected the upper and lower respiratory tracts (31–33). In addition, alveolar type II pneumocytes are the same target cells for both IAV and SARS-CoV-2 even though they have different entry cellular receptors (32, 34, 35). Thus, coinfection is highly possible especially when these two viruses are circulating at the same time. A respective study showed that the coinfection rate of SARS-CoV-2 and IAVs was as high as 49.8% in a single-centered study of 307 COVID-19 patients during the outbreak period in Wuhan (36). Meanwhile, another study based on surveillance in the United Kingdom also showed that 19% of COVID-19 patients were tested positive for both IAV and SARS-CoV-2 when COVID-19 was first emerged in the U.K. from January to April 2020 (37). Given the high coinfection rate of those two viruses, the impact of COVID-19 alongside

influenza on morbidity and mortality is a major concern in the 2021 to 2022 flu season in the Northern hemisphere.

In this study, we examined the disease outcomes in ferrets coinfecting with SARS-CoV-2 and IAVs and the ability of the seasonal influenza virus vaccine to protect against disease and transmission.

## RESULTS

**IAV and SARS-CoV-2 coinfection enhanced the disease severity in ferrets.** To determine the effect of SARS-CoV-2 and IAV coinfections, ferrets were infected with either IAV or SARS-CoV-2 alone or together and served as naive transmitter ferrets (Fig. 1A). At 1 d postinfection (pi), nasal washes were performed on each naive transmitter ferret before cohousing with a receiver ferret. The naive transmitter ferrets were monitored for bodyweight loss and the ability to transmit the viruses to receiver ferrets over 14 days (Fig. 1A). As shown in Fig. 1B, SARS-CoV-2 single-infected ferrets did not lose any body weight during the 14 days of observation, H1N1 CA/09 single-infected ferrets lost an average ~10% of their body weight (range was 5 to 15% of original body weight) by 7 d pi and then began to recover, which is consistent with a previous observation (38), while SARS-CoV-2 and CA/09 coinfecting ferrets lost an average of 18% their body weight by 7 d pi (14 to 21%), which was significantly lower than either CA/09 or SARS-CoV-2 single-infected ferrets (Fig. 1B). The coinfecting ferrets also recovered slowly and did not return to their full body weight during the observation period (Fig. 1B). The same disease enhancement was observed in ferrets coinfecting with SARS-CoV-2 and KS/17 (H3N2) viruses. Ferrets infected with the KS/17 virus lost little weight over the 14 days while ferrets coinfecting with SARS-CoV-2 and KS/17 lost between 3% and 10% of their body weight, which was statistically lower than KS/17 single-infected ferrets at 14 d pi (Fig. 1B).

Receiver ferrets began to lose weight by 3 to 5 d postexposure (pe) except for receiver ferrets cohoused with SARS-CoV-2 single-infected transmitter ferrets (Fig. 1C). Receiver ferrets cohoused with CA/09 single-infected or CA/09 and SARS-CoV-2 coinfecting transmitter ferrets lost a statistically similar percentage of weight postexposure (Fig. 1C). In comparison, receiver ferrets cohoused with KS/17 and SARS-CoV-2 coinfecting transmitter ferrets lost significantly more body weight than KS/17 or SARS-CoV-2 single-infected ferrets (Fig. 1C).

**IAV transmitted more efficiently than SARS-CoV-2 by direct contact in ferrets.** To evaluate virus shedding and transmission by direct contact for both IAVs and SARS-CoV-2, virus titers in nasal washes collected from both transmitter ferrets and receiver ferrets were assessed. IAVs were detectable from all transmitter ferrets from nasal washes collected at 1, 3, and 5 d pi, the viruses were completely cleared from nasal washes by 7 d pi (Fig. 2A to D). The IAV mean virus titers in the coinfecting ferrets were lower than those in IAV single-infected ferrets. However, the SARS-CoV-2 virus was only detectable at 1 d pi in the coinfecting transmitter ferrets (Fig. 2E and F) while the virus was detectable for up to 5 d pi in SARS-CoV-2 virus single-infected transmitter ferrets (Fig. 2G).

IAV is transmitted efficiently by direct contact in ferrets. Receiver ferrets cohoused with CA/09 single-infected or CA/09 and SARS-CoV-2 coinfecting transmitter ferrets had similar viral titers compared to their transmitter ferrets (Fig. 2H and I). However, there was a delay in the detection of the KS/17 virus in the receiver ferrets compared to the transmitter ferrets (Fig. 2J and K). Receiver ferrets cohoused with KS/17 single-infected transmitter ferrets had no detectable virus titers at 2 d pe but had high detectable virus titer at 4, 6, or 8 d pe (Fig. 2J), while the receiver ferrets cohoused with KS/17 and SARS-CoV-2 coinfecting transmitter ferrets initially had high detectable virus titer from 4 d pe, and the virus was cleared from nasal washes by 8 d pe (Fig. 2K).

However, SARS-CoV-2 did not transmit as efficiently as IAVs in ferrets. SARS-CoV-2 was undetectable in receiver ferrets cohoused with coinfecting transmitter ferrets (Fig. 2L and M), SARS-CoV-2 was only detected in receiver ferrets cohoused with SARS-CoV-2 single-infected transmitter ferrets within the first 6 d pe (Fig. 2N).

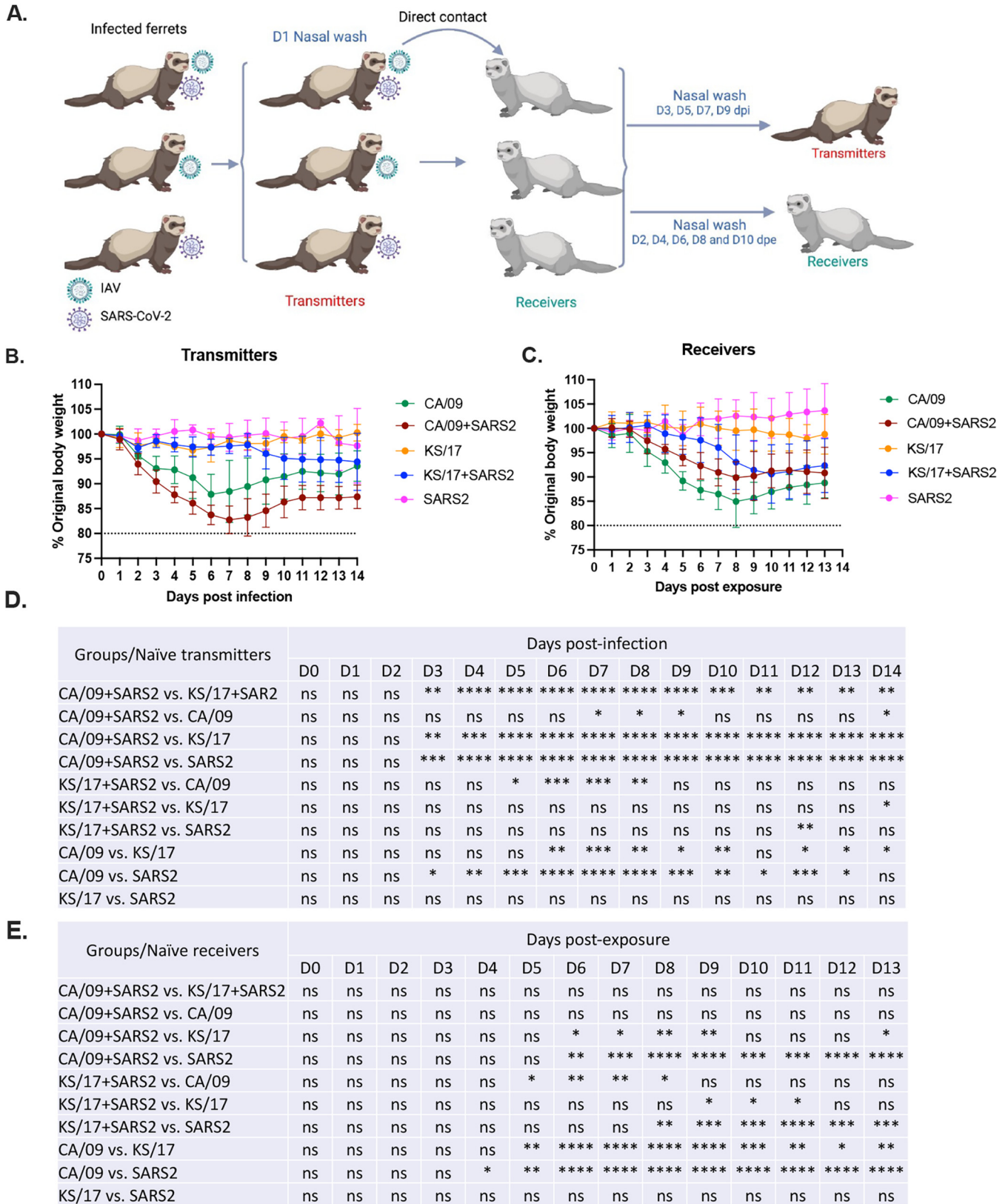


**FIG 1** Schematic of IAV and SARS-CoV-2 coinfection in naïve transmitter ferrets and transmission by direct contact. (A). Schematic coinfection and transmission experiment layout. Ferrets ( $n = 16$ ) were coinfecting with IAV (H1N1 or H3N2) and SARS-CoV-2 simultaneously or singly infected with IAV or SARS-CoV-2 (naïve transmitters). At 1 d pi, nasal washes were performed and another set of naïve ferrets ( $n = 16$ ) (receivers) were cohoused with infected transmitter ferrets. Nasal washes were performed at 3, 5, 7, and 9 d pi from transmitter ferrets, and 2, 4, 6, 8, 10 d pe from receiver ferrets for viral titration. (Continued on next page)

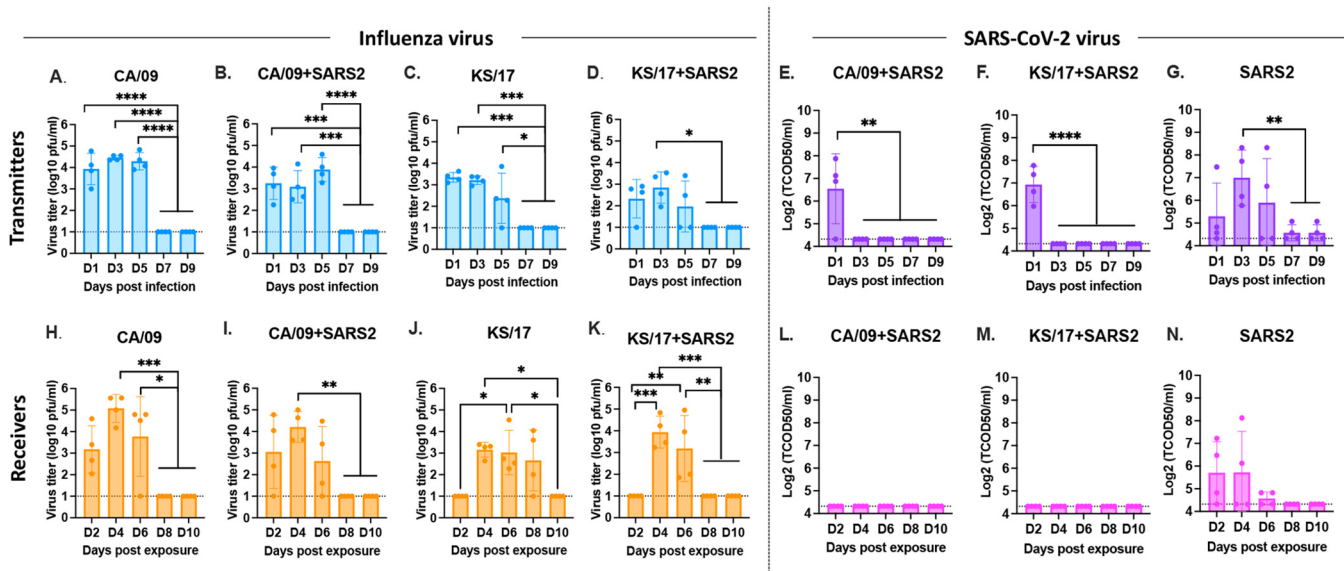


**FIG 2** IAV and SARS-CoV-2 viral titers from nasal washes. IAV and SARS-CoV-2 nasal wash viral titers were assessed in both naive transmitter ferrets and their receiver ferrets at different time points postinfection/exposure. (A to D). IAV viral titers or SARS-CoV-2 viral titers (E to G) in naive transmitter ferrets postinfection. (H to K). IAV viral titers or SARS-CoV-2 viral titers (L to N) in naive receiver ferrets postexposure. IAV viral titers were determined by plaque forming assay and presented as PFU per milliliter (PFU/mL), and SARS-CoV-2 viral titers were determined by median tissue culture infectious dose (TCID<sub>50</sub>) and presented as TCID<sub>50</sub>/mL. The dotted line indicated the limit of detection. Statistical differences of viral titers on different time points postinfection were analyzed using a one-way ANOVA and indicated as asterisks: \*, *P* < 0.05; \*\*, *P* < 0.01; \*\*\*, *P* < 0.001; \*\*\*\*, *P* < 0.0001.

To access the lung viral titers in the naive transmitter ferrets after a single infection or coinfection, ferrets were euthanized, and the lung tissue was collected at 4 d pi. Approximately 10<sup>4</sup> to 10<sup>6</sup> plaque forming unit (PFU)/mL of IAVs was detected in ferrets single-infected with CA/09 or coinfecting with CA/09 and SARS-CoV-2, and the viral titers were statistically similar between those two groups (Fig. 3A). No IAVs were detected in ferrets single-infected with KS/17 or SARS-CoV-2 alone or coinfecting with KS/17 and SARS-CoV-2 (Fig. 3A). Moreover, no infectious SARS-CoV-2 was detected in the ferret regardless of whether they were singly infected with SARS-CoV-2 or coinfecting with IAV (Fig. 3B), indicating that KS/17 and SARS-CoV-2 infected or replicated efficiently in the upper but not the lower respiratory tract in ferrets.

**IAV and SARS-Cov-2 coinfection induced more severe inflammation in nasal cavities and lungs.** To further access the histopathological changes in experimentally infected ferrets, naive ferrets that were directly infected with either IAV alone or coinfecting with SARS-CoV-2, ferrets (*n* = 3/group) were euthanized on 4 d pi, and the nasal cavity and lung tissue were collected and fixed in formalin for hematoxylin and eosin (H&E) staining. It was a single point of time in an infection, and the kinetics of histologic changes could be different for different viruses and the viral combination. In the nasal cavity, a single infection with SARS-CoV-2, CA/09, or KS/17 induced minimal to mild inflammation (Fig. 4A, C, D to F). However, CA/09 and SARS-CoV-2 coinfection induced significantly more severe inflammation than CA/09 or SARS-CoV-2 infection alone (Fig. 4A, C, F to G), and KS/17 and SARS-CoV-2 coinfection also resulted in statistically higher inflammation than KS/17 or SARS-CoV-2 infection alone (Fig. 4A, C to E). In the lungs, the same phenomenon was observed. CA/09 and SARS-CoV-2 coinfection induced more severe inflammation than CA/09 or SARS-CoV-2 infection alone (Fig. 4B, H, K to L), but the inflammation scores were not statistically different between KS/17 and SARS-CoV-2 coinfection and KS/17 infection alone (Fig. 4B, H to J).

**FIG 1 Legend (Continued)**

All the ferrets were monitored for body weight and mortality for 14 days postinfection/postexposure. (B) Bodyweight curve of infected transmitter ferrets. (C). Bodyweight curve of receiver ferrets. The dotted line indicated 80% of original body weights. Statistical differences in body weight between different groups were analyzed using two-way ANOVA. (D). Statistical analysis of body weight loss between naive transmitter ferrets postinfection. (E). Statistical analysis of body weight loss between naive receiver ferrets postexposure. Statistical differences were indicated as asterisks: \*, *P* < 0.05; \*\*, *P* < 0.01; \*\*\*, *P* < 0.001; \*\*\*\*, *P* < 0.0001.

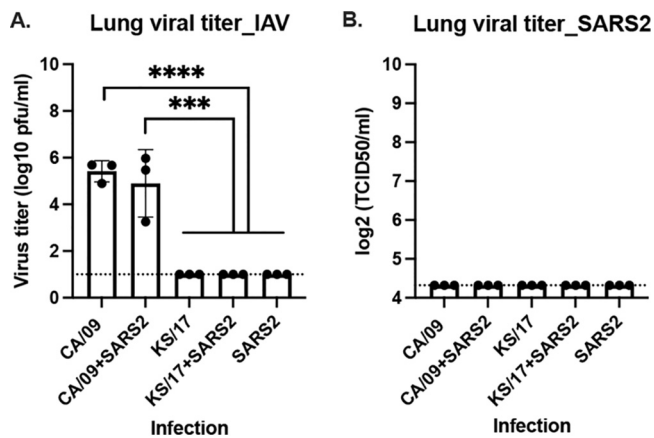


**FIG 3** IAV and SARS-CoV-2 viral titers in lung tissues. Naïve ferrets were either single-infected with IAV or SARS-CoV-2 or coinfecting with those two viruses simultaneously. On 4 d pi, lung tissues were collected for viral titration. (A) IAV viral titers were determined by plaque forming assay and presented as PFU per milliliter (PFU/mL). (B). SARS-CoV-2 viral titers were determined by median tissue culture infectious dose (TCID<sub>50</sub>) and presented as TCID<sub>50</sub>/mL. The dotted line indicated the limit of detection. Statistical differences of lung viral titers between groups were analyzed using a two-way ANOVA and indicated as asterisks: \*,  $P < 0.05$ ; \*\*,  $P < 0.01$ ; \*\*\*,  $P < 0.001$ ; \*\*\*\*,  $P < 0.0001$ .

**Seasonal influenza vaccine ameliorated the disease severity caused by IAV and SARS-CoV-2 coinfection in ferrets.** To determine if seasonal influenza vaccine will reduce the disease severity induced by the coinfection of IAVs and SARS-CoV-2, a subset of ferrets was intramuscularly vaccinated with the 2019 to 2020 split-inactivated Fluzone seasonal influenza vaccine (Sanofi Pasteur, Swiftwater, PA, USA) twice and then infection and direct contact transmission were performed (Fig. 5A). All the vaccinated ferrets seroconverted to each of the vaccine components by 42 d after initial vaccination (Fig. 6), and the hemagglutinin antibody inhibition (HAI) titers against CA/09 (not a vaccine component) and Bris/18 were statistically identical (Fig. 6A and B). Vaccinated transmitter ferrets that were single infected with CA/09 lost ~10% of their body weight by 6 d pi (Fig. 5B, solid circle), which was significantly lower than the CA/09 infected naïve transmitter ferrets without any vaccination (Fig. 5B, open circle). While vaccinated transmitter ferrets that coinfecting with CA/09 and SARS-CoV-2 (Fig. 5C, red solid circle) also lost significantly lower body weight (~5%) than the naïve transmitter ferrets (Fig. 5C, open circle). Those vaccinated transmitter ferrets were rapidly recovered to their original body weight while the naïve transmitter ferrets did not recover their body weight by 14 d pi (Fig. 5C, solid circle). In contrast, the KS/17 or SARS-CoV-2 infection was mild in ferrets, and single-infected or coinfecting vaccinated transmitter ferrets either maintained their body weight or gained 5% of their body weight for the entire 2 weeks (Fig. 5D to F). However, there was still a trend that the vaccinated transmitters had a higher mean body weight (color solid circle) than the naïve transmitter ferrets (open circle) at all time points after infection.

The receiver ferrets cohoused with CA/09 single-infected vaccinated transmitter ferrets (Fig. 5G, solid circle) lost ~10% of their body weight during the exposure, and statistically similar body weight loss was also observed in the receiver ferrets cohoused with CA/09 and SARS-CoV-2 coinfecting vaccinated transmitter ferrets (Fig. 5H, solid circle). As we observed, no statistically different body weight loss was observed between receiver ferrets cohoused with vaccinated transmitter ferrets (Fig. 5G and H, solid circle) and naïve transmitter ferrets (Fig. 5G and H, open circle) after infection. However, receiver ferrets cohoused with either KS/17 infected vaccinated transmitter ferrets (Fig. 5I, solid circle) or KS/17 and SARS-CoV-2 coinfecting vaccinated transmitter ferrets (Fig. 5J, solid circle) did not lose any body weight during the whole time of exposure. The receiver ferrets were cohoused with naïve transmitter ferrets that were either infected with KS/17 or coinfecting with KS/17 and SARS-CoV-2 lost (Fig. 5I and J, open circle) significantly more body weight than those cohoused with the

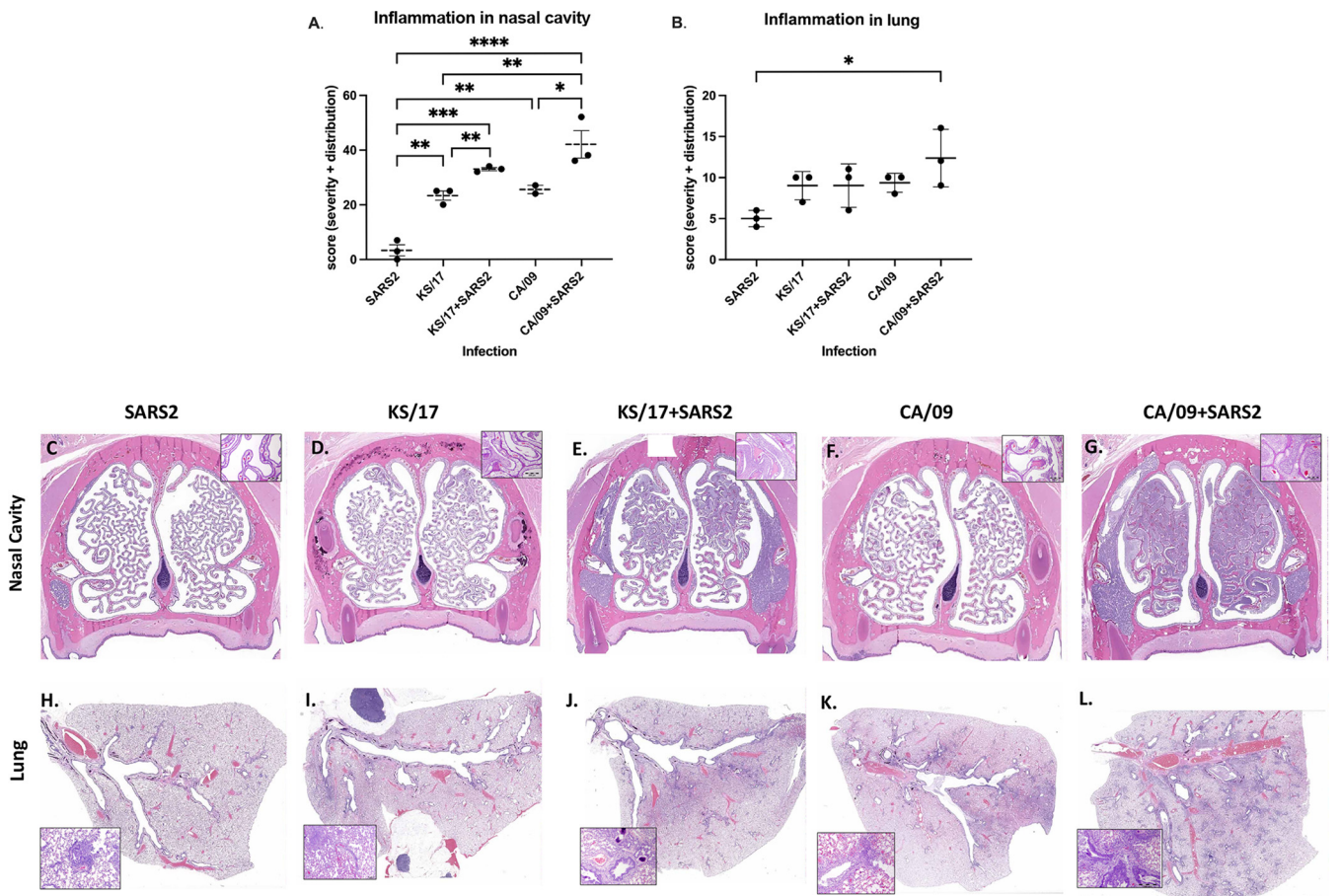


**FIG 4** Inflammation in nasal cavity and lungs of single-infected or coinfecting ferrets. Ferrets were either single-infected with IAV or SARS-CoV-2 or coinfecting with those two viruses simultaneously. On 4 d pi, the nasal cavity and lungs from three ferrets in each group were collected for histopathological analysis. (A and B) Inflammation score in the nasal cavity (A) and lungs (B) after single infection or coinfection. (C to L) Representative images of noses and lungs histopathological changes at 4 d pi after single infection or coinfection. The boxed area is magnified showing inflammatory cells infiltration. Lesion severity and distribution were evaluated and scored: 0 = no histological change; lesion severity: 1 = minimal, 2 = mild, 3 = moderate, 4 = severe; lesion distribution: 1 = focal, 2 = multifocal, 3 = diffuse. Statistical differences of inflammation scores between groups were analyzed using a one-way ANOVA and indicated as asterisks: \*,  $P < 0.05$ ; \*\*,  $P < 0.01$ ; \*\*\*,  $P < 0.001$ ; \*\*\*\*,  $P < 0.0001$ .

corresponding vaccinated transmitter ferrets after infection (Fig. 5I and J, solid circle). In contrast, receiver ferrets exposed to SARS-CoV-2 infected naive/vaccinated transmitter ferrets did not lose any body weight during the observation period (Fig. 5K).

**Influenza virus vaccine did not completely block IAV direct contact transmission but shortened the shedding period with lower virus titer in ferrets.** To determine whether the seasonal influenza vaccine affected IAVs and SARS-CoV-2 infection and direct contact transmission, both IAVs and SARS-CoV-2 viral nasal wash titers were assessed from vaccinated transmitter ferrets and their receiver ferrets at different time points postinfection/exposure.

In the vaccinated transmitter ferrets, CA/09 was detectable in nasal washes at 1 and 3 d pi (Fig. 7A and B) after single-infection with CA/09 and coinfection with SARS-CoV-2 simultaneously, and the virus titers were significantly lower in those vaccinated transmitter ferrets compared to that in naive transmitter ferrets. While KS/17 virus was only detectable at 1 d pi in vaccinated transmitter ferrets after single-infection with KS/17, and KS/17 was retrieved at 1 and 3 d pi in vaccinated transmitter ferrets after coinfection with KS/17 and SARS-CoV-2 (Fig. 7C), suggesting IAV (CA/09 and KS/17) shedding was shortened by at least 2 days in vaccinated transmitter ferrets compared to the naive simultaneously (Fig. 7A to D). However, SARS-CoV-2 was barely detectable at any time point in the vaccinated transmitter ferrets after coinfection (Fig. 7E and F), the virus was only detectable in 1 ferret at 1 d pi and in 2 ferrets at 5 d pi in the vaccinated

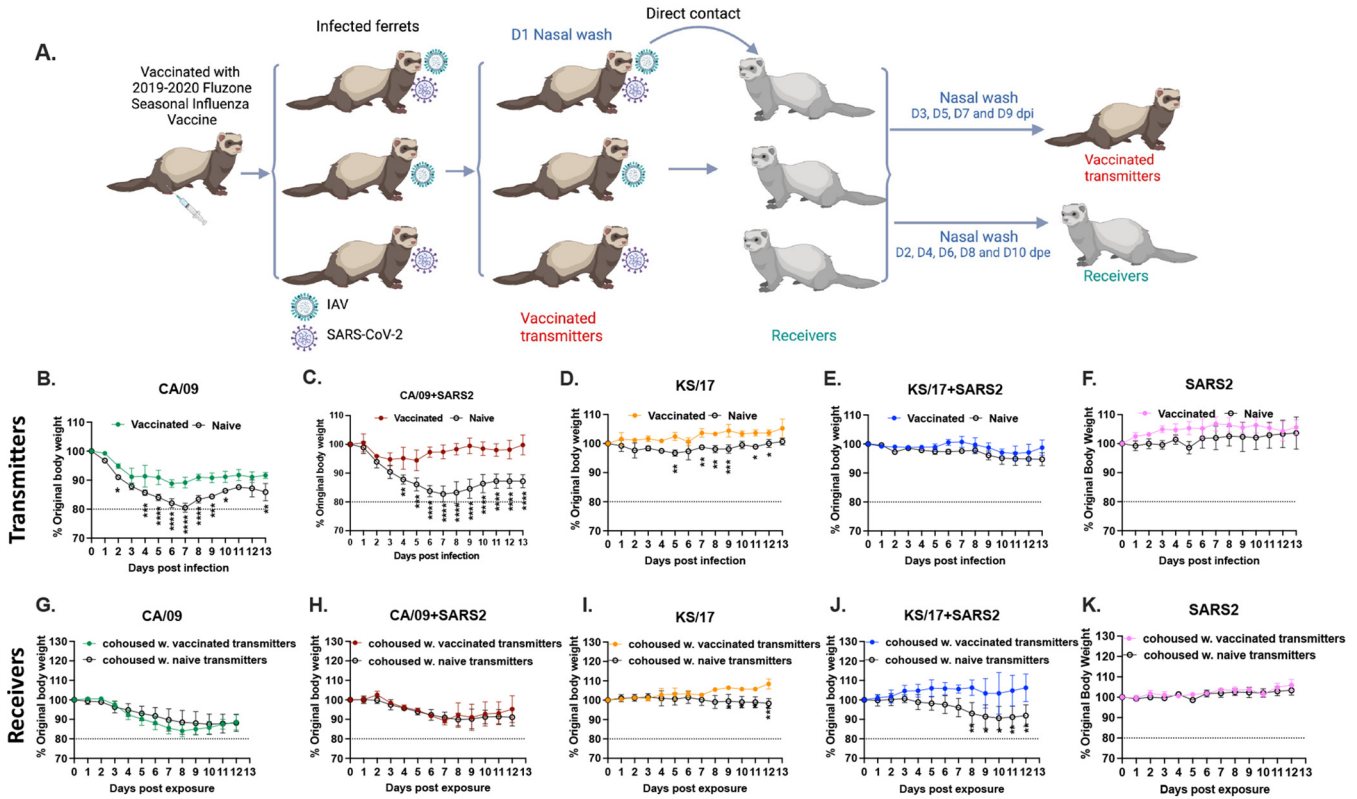


**FIG 5** Schematic of IAV and SARS-CoV-2 coinfection in Fluzone vaccinated transmitter ferrets and transmission by direct contact (A). Ferrets ( $n = 15$ ) were intramuscularly vaccinated with the 2019 to 2020 Fluzone quadrivalent influenza vaccine at days 0 and 28 ( $250 \mu\text{L}/\text{dose}$ ). At day 56, vaccinated ferrets were coinfecting with IAV (H1N1 or H3N2) and SARS-CoV-2 simultaneously or single-infected with either IAV or SARS-CoV-2 (vaccinated transmitters). On 1 d pi, nasal washes were performed on those vaccinated transmitter ferrets and another set of naive ferrets ( $n = 15$ ) (receivers) were cohoused with vaccinated transmitter ferrets. Nasal washes were collected at 1, 3, 5, 7, and 9 d pi from vaccinated transmitter ferrets, and at 2, 4, 6, 8, 10 d pe from receivers for viral titration. All ferrets are monitored for body weight loss for 14 days postinfection. (B-F) Bodyweight curves of the vaccinated transmitter ferrets were compared to the naive transmitter ferrets that were: single-infected with CA/09 (B); coinfecting with CA/09 and SARS-CoV-2 (C); single-infected with KS/17 (D); coinfecting with KS/17 and SARS-CoV-2 (E); single-infected with SARS-CoV-2 (F). (G to K) Bodyweight curves of receiver ferrets that were cohoused with vaccinated transmitter ferrets were compared to the naive transmitter ferrets that were: single-infected with CA/09 (G); coinfecting with CA/09 and SARS-CoV-2 (H); single-infected with KS/17 (I); coinfecting with KS/17 and SARS-CoV-2 (J); single-infected with SARS-CoV-2 (K). The dotted line indicated 80% of original body weights. Statistical differences of body weight between groups were analyzed using a two-way ANOVA and indicated as asterisks: \*,  $P < 0.05$ ; \*\*,  $P < 0.01$ ; \*\*\*,  $P < 0.001$ ; \*\*\*\*,  $P < 0.0001$ .

transmitter ferrets after coinfection with KS/17 and SARS-CoV-2 (Fig. 7F), but the virus was detectable in SARS-CoV-2 single-infected ferrets up to 5 d pi and was detectable in all ferrets at 3 d pi (Fig. 7G).

Receiver ferrets cohoused with CA/09 single-infected or CA/09 and SARS-CoV-2

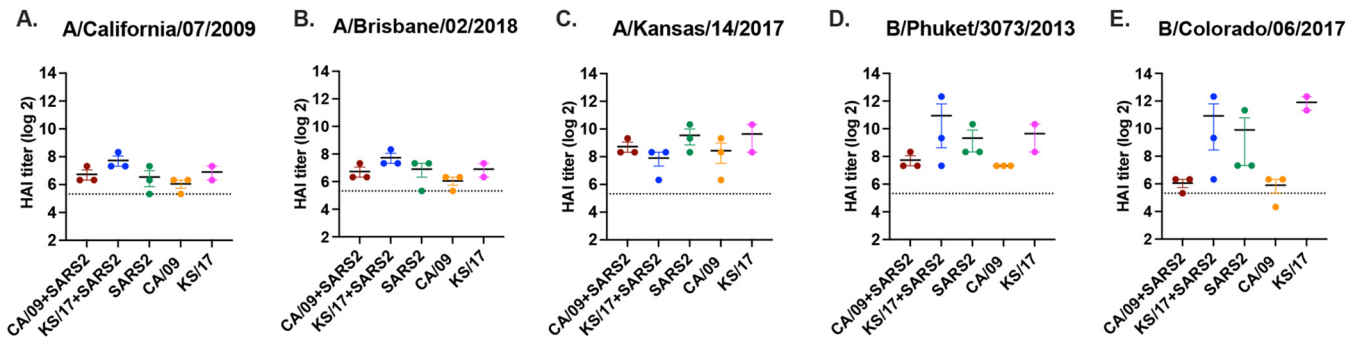


**FIG 6** Hemagglutination inhibition serum antibody titers induced by Fluzone quadrivalent vaccine in vaccinated ferrets. HAI titers were determined for ferrets ( $n = 15$ ) that were intramuscularly vaccinated twice (days 0 and 28) with  $250 \mu\text{L}$  of the 2019 to 2020 Fluzone quadrivalent seasonal influenza vaccine. Antisera were collected at day 42 post-initial vaccination for HAI assay against vaccine virus components as well as A/California/07/2009 virus. Values are the individual animal HAI titers: (A) A/California/07/2009 (H1N1); (B) A/Brisbane/02/2018 (H1N1); (C) A/Kansas/14/2017 (H3N2); (D) B/Phuket/3073/2013 (B-Vic); (E) B/Colorado/06/2017 (B-Yam). The dotted line indicated the 1:40 HAI titer.

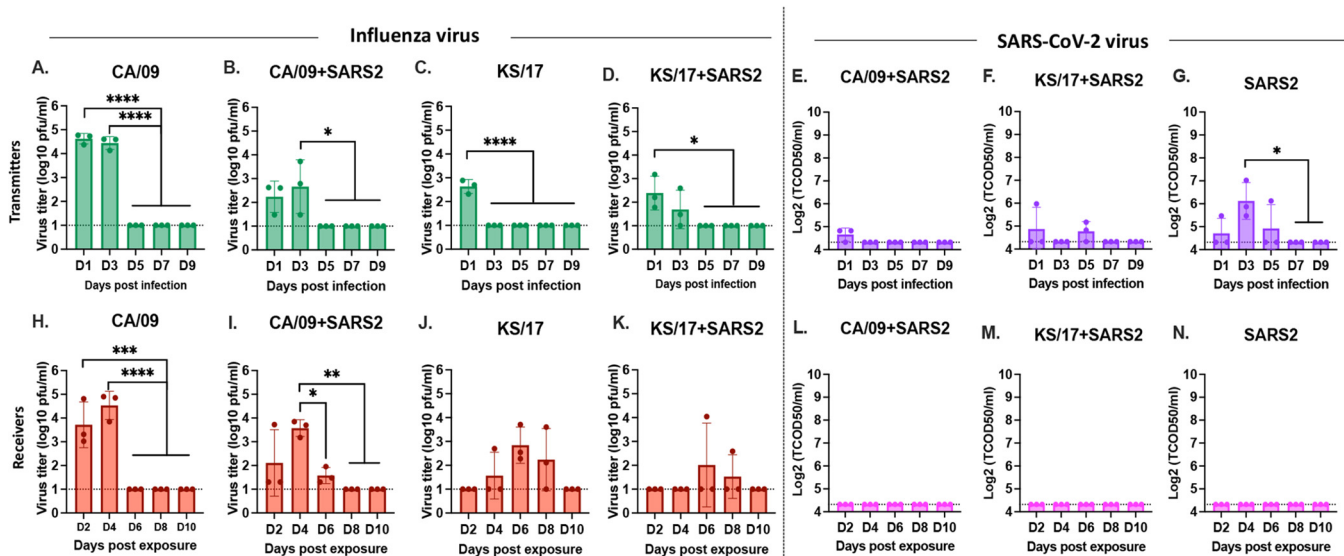


**FIG 7** IAV and SARS-CoV2 virus titers from nasal washes. IAV and SARS-CoV-2 nasal wash viral titers were assessed in both vaccinated transmitter ferrets and their naive receiver ferrets at different time points postinfection/postexposure (A to D). IAV viral titers or SARS-CoV-2 viral titers (E to G) in vaccinated transmitter ferrets postinfection. (H to K). IAV viral titers or SARS-CoV-2 viral titers (L to N) in naive receiver ferrets postexposure. IAV viral titers were determined by plaque forming assay and presented as PFU per milliliter (PFU/mL), and SARS-CoV-2 viral titers were determined by median tissue culture infectious dose (TCID<sub>50</sub>) and presented as TCID<sub>50</sub>/mL. The dotted line indicated the limit of detection. Statistical differences of viral titers on different time points postinfection were analyzed using a two-way ANOVA and indicated as asterisks: \*, *P* < 0.05; \*\*, *P* < 0.01; \*\*\*, *P* < 0.001; \*\*\*\*, *P* < 0.0001.

coinfected vaccinated transmitter ferrets had similar virus titers as the directly infected vaccinated transmitter ferrets (Fig. 7H and I). In contrast, there was a delay in detecting KS/17 with virus titers peaking at 6 d pe, and the virus was still detectable in receiver ferrets until 8 d pe (Fig. 7J and K). Importantly, lower mean viral titers were observed in receiver ferrets that were cohoused with vaccinated transmitter ferrets than those cohoused with naive transmitter ferrets. However, no receiver ferrets had detectable SARS-CoV-2 virus titer at any time point postexposure with vaccinated transmitter ferrets (Fig. 7L to N). Despite no live SARS-CoV-2 virus detected in the nasal washes of the receiver ferrets, the viral RNA (vRNA) could be detected in the receiver ferrets that cohoused with SARS-CoV-2 single-infected vaccinated transmitter ferrets at day 3 d pi, but not those cohoused with IAVs and SARS-CoV-2 coinfecting vaccinated transmitter ferrets (Fig. 8).

**DISCUSSION**

Influenza viruses cause ~5 million cases of severe illness and 290,000 to 650,000 deaths worldwide per year (39). In the U.S., there are ~36,000 deaths and more than 200,000 hospitalizations annually (40) with an average annual economic cost greater than \$11 billion (41). Infection with influenza virus does not preclude coinfection with a second pathogen. Both influenza A viruses and SARS-CoV-2 have been cocirculated since the 2019 to 2020 influenza seasons, and there have been documented cases of coinfections with these two viruses (36, 42–47). Along with the SARS-CoV-2 virus continuously circulating, it will be more challenging in this 2021 to 2022 influenza season in the Northern Hemisphere. Coinfection cases have ranged from mild to severe in clinical outcome with some cases not significantly worse than infection with SARS-CoV-2 or influenza virus alone (48), whereas other coinfection cases had more severe disease (46, 49). In this study, we used the well-established ferret model for influenza virus infection to examine coinfection with the SARS-CoV-2 virus.

In this study, we demonstrated that SARS-CoV-2 and IAVs (H1N1 and H3N2) coinfection enhanced the disease severity in ferrets, and the coinfection induced more severe inflammation in the upper respiratory tract as well as in lungs than the single infection in ferrets, which is consistent with the coinfection studies performed in ACE2

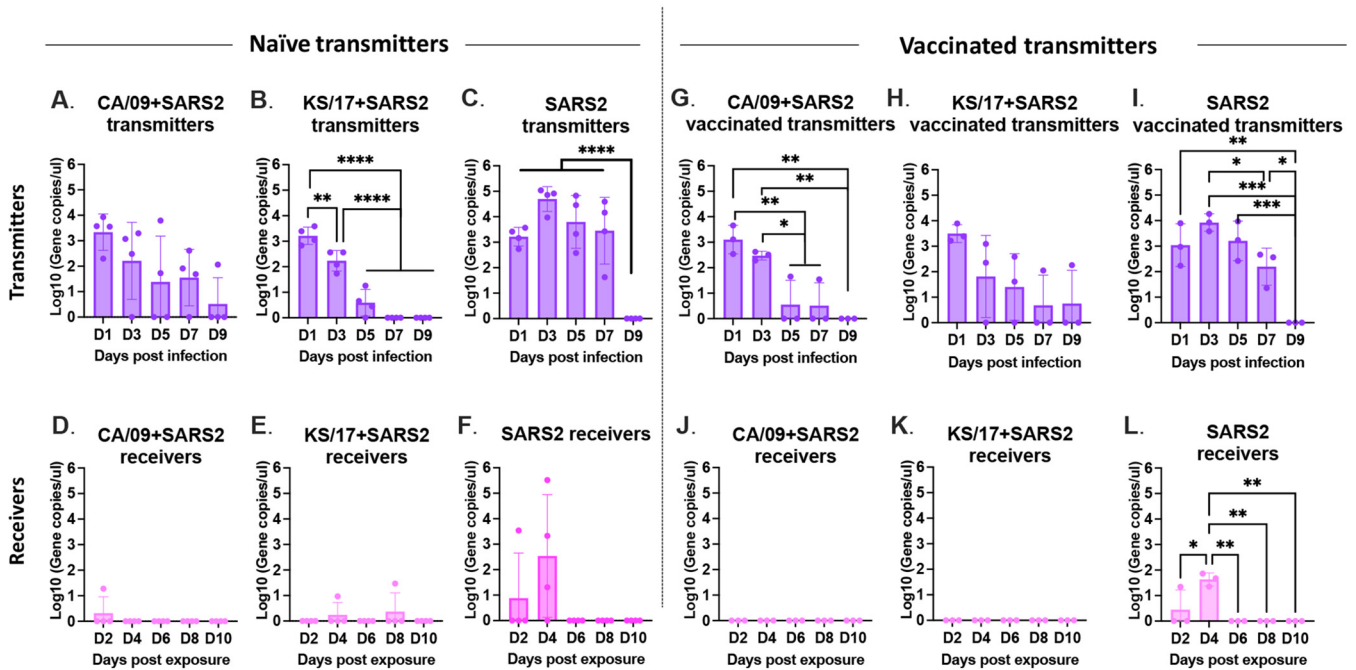


**FIG 8** SARS-CoV-2 viral RNA level from nasal washes. SARS-CoV-2 viral N gene was detected by RT-qPCR in nasal washes collected from: (A and B) coinfecting naïve transmitter ferrets; (C) SARS-CoV-2 infected naïve transmitter ferrets; (D and E) receiver ferrets cohoused with coinfecting naïve transmitter ferrets; (F) receiver ferrets cohoused with SARS-CoV-2 infected naïve transmitter ferrets; (G-H) coinfecting vaccinated transmitter ferrets; (I) SARS-CoV-2 infected vaccinated transmitter ferrets; (J and K) receiver ferrets cohoused with coinfecting vaccinated transmitter ferrets; (L) receiver ferrets cohoused with SARS-CoV-2 infected vaccinated transmitter ferrets. Statistical differences were analyzed using a one-way ANOVA and indicated as asterisks: \*,  $P < 0.05$ ; \*\*,  $P < 0.01$ ; \*\*\*,  $P < 0.001$ ; \*\*\*\*,  $P < 0.0001$ .

transgenic mice and hamsters (24, 50–52). As we noticed, SARS-CoV-2 infection was very mild in ferrets and no clinical alterations in body weight were observed, but when ferrets were coinfecting with IAV (a subtype of H1N1 or H3N2), the disease was more severe than either single infection by IAV or SARS-CoV-2, and coinfecting ferrets lost significantly more body weight compared to single-infected animals. Ferrets are susceptible to experimental infection of SARS-CoV-2, and the infection is dose-dependent, virus shedding is undetectable when the infectious dose is low (53). However, ferrets are semipermissive to natural infection by direct contact, and no infection was detected by droplet transmission (54). In contrast, IAV single infection (CA/09 H1N1) did not cause any body weight loss in hamsters, while IAV and SARS-CoV-2 coinfection caused hamsters to lose 9.6% of their body weight at 4 d postinfection (24). Although we observed the coinfection enhanced the diseases in both ferrets and hamsters, IAVs and SARS-CoV-2 had different susceptibilities to these two animal models. In ferrets, IAV infection is more efficient than SARS-CoV-2, IAV infection was associated with high virus titer detected from nasal washes no matter infection alone or coinfection with SARS-CoV-2, but SARS-CoV-2 infection had significantly lower virus titer detected after coinfection, and virus shedding was only detectable in the first 1 to 3 d postinfection. In contrast, hamsters are more susceptible to SARS-CoV-2 than IAV (24). The SARS-CoV-2 virus replicated rapidly in both upper and lower respiratory and viral titer peaked at 4 d pi, while IAV infection was not as efficient as SARS-CoV-2. Even though a high dose of IAV was used for infection, only little viruses could be detected from the upper respiratory tract in hamsters (24). However, ACE2 transgenic mice are highly susceptible to both IAV and SARS-CoV-2, high viral titers for both viruses could be detected in both upper and lower respiratory tracts, and the coinfection with a nonlethal dose of IAV and SARS-CoV-2 also aggravated the pathogenesis and led to 100% mortality (50–52). Lei et al. (50) reported that coinfection with IAV enhanced SARS-CoV-2 infectivity in ACE2 transgenic mice, but the enhanced SARS-CoV-2 infectivity facilitated by IAV was not observed in Achdout et al. (51), which showed SARS-CoV-2 infectivity was

interrupted by coinfection with IAV in the ACE2 transgenic mouse model. Moreover, similar SARS-CoV-2 infection interference caused by coinfection with IAV was also observed in ferrets and hamsters (24).

IAV and SARS-CoV-2 may compete during coinfection in ferrets, hamsters, and ACE2 transgenic mice considering IAVs and SARS-CoV-2 infect the same target cells in the respiratory tract (51, 55–59). There was evidence of pathogenic competition between IAV and seasonal coronaviruses (60). Moreover, another study in the U.K. also revealed that the risk of testing positive for SARS-CoV-2 was 68% lower among influenza-positive cases (37). In this study, we found that SARS-CoV-2 was only detectable on 1 d pi in coinfecting ferrets but detectable until 5 d pi in SARS-CoV-2 single-infected ferrets. Similarly, the potential competitive infection was also observed in hamsters and transgenic ACE2 mice (24), lower SARS-CoV-2 virus loads were observed when coinfection with those two viruses compared to a single infection with SARS-CoV-2 (24, 51). We only examined simultaneous coinfection in this study, but sequential infection may yield similar results (24, 52). Previously our group demonstrated that in influenza sequential coinfections, the elicitation of innate immune responses reduces the ability of the second virus to productively infect the same ferret, and often a 60 to 90 days rest period is necessary to achieve sequential viral infections (38).

IAVs transmitted efficiently in ferrets by direct contact as we demonstrated in this study, and IAV titers in receiver ferrets were as high as titers in their cohoused transmitter ferrets, suggesting that IAV transmission was not interrupted by SARS-CoV-2. However, SARS-CoV-2 virus transmission was influenced when IAV existed, and the transmission efficacy was significantly low between ferrets. No infectious SARS-CoV-2 virus could be detected from the receiver ferrets that were exposed to the coinfecting transmitter ferrets, and the infectious virus was only detectable in the receiver ferrets that were exposed to SARS-CoV-2 single-infected transmitter ferrets. Because coinfection made SARS-CoV-2 virus shedding shortened to 1 day postinfection and nasal washes were also performed on those transmitter ferrets at 1 d pi, which resulted in little to no virus could be transmitted to the receiver ferrets. In addition, SARS-CoV-2 virus shedding in the upper respiratory tract is dependent on the initial infection dose (53), a low infection dose might lead to no virus detectable in ferrets. Although SARS-CoV-2 transmission between ferrets had been documented by measuring viral RNA levels in the receiver ferrets, no infectious virus could be isolated (26, 27, 53, 61).

Seasonal influenza virus vaccination significantly reduced the IAV titers, thus ameliorating the disease severity in ferrets no matter a single infection with IAV or coinfection with IAV and SARS-CoV-2. Moreover, influenza virus vaccination shortened IAV shedding from the infected ferrets. Even though the virus transmission was not completely blocked by vaccination, lower IAV titers, shorter shedding time, and delayed virus titer peak was found in receiver ferrets. The severity of disease induced by coinfection was predominantly contributed by IAV in the ferret, getting IAV under control significantly improved the disease outcome. Influenza immunity prevented severe manifestations in coinfecting ACE2 transgenic mice were also reported (51, 52). Although SARS-CoV-2 infection caused very mild disease in ferrets, coinfection with IAV showed severe exacerbation, therefore, we speculated that COVID-19 vaccination might also alleviate the disease severity in coinfecting ferrets, which will need to be further determined. Achdout et al. (51) reported that SARS-CoV-2 immunity did not prevent increased lethality induced in ACE-2 transgenic mice, but SARS-CoV-2 immunity may prevent the severe diseases in hamsters because the enhanced diseases after coinfection was predominantly led by SARS-CoV-2 infection in hamsters, which should be ameliorated once SARS-CoV-2 infection got controlled (24). In addition, different challenge stocks of the SARS-CoV-2 virus were used in different studies, which may have contributed to the considerable variations.

Overall, our results demonstrated the positive effect of seasonal influenza virus vaccination on reducing the effects of not only IAV induced disease, but also the effects of IAV and SARS-CoV-2 coinfection. As the Northern hemisphere entered flu season, SARS-CoV-2 variants are still circulating, more documented coinfections will continue

to grow in the human population. Therefore, it is necessary to get seasonal influenza vaccination for reducing the risk of severe morbidity of influenza/COVID-19 coinfection during the COVID-19 pandemic and add benefits for overall public health by preventing viral infection, reducing viral transmissions, decreasing hospital visitations, and reducing the complications of COVID-19 lockdowns and restrictions, particularly for high-risk populations (23, 24).

## MATERIALS AND METHODS

**Cells and viruses.** Madin-Darby canine kidney (MDCK) cells and Vero-E6 cells were maintained in Dulbecco's modified Eagle's medium (DMEM) supplemented with 10% fetal bovine serum (FBS) and 1% penicillin-streptomycin solution (10,000 U/mL) at 37°C with 5% CO<sub>2</sub>. Influenza A and B viruses used in this study were grown in eggs. The A/California/07/2009 (H1N1) was obtained from Virapur (NY, USA), A/Kansas/14/2017 (H3N2), B/Phuket/3073/2013 (B-Vic), and B/Colorado/06/2017 (B-Yam) were obtained from International Reagent Resource (IRR). The SARS-CoV-2 virus isolate, USA-WA1/2020, was originally purchased from BEI resources. The SARS-CoV-2 virus was grown in Vero E6 cells and passaged three times and this stock of virus was used for infection. All experiments involving live SARS-CoV-2 virus were performed in the Biosafety Level-3 (BSL-3) facility at the University of Georgia (UGA) following approved standard operating procedures.

**Animals.** Fitch ferrets (*Mustela putorius furo*, female, 6 to 15 months of age), negative for antibodies to circulating influenza A (H1N1 and H3N2) influenza B viruses and SARS-CoV-2 virus, were descended and purchased from Triple F Farms (Gillett, PA, USA). Ferrets were pair housed in stainless steel cages (Shor-Line) containing Sani-Chips laboratory animal bedding and allowed free access to food and water. They were cared for under USDA guidelines for laboratory animals. All procedures were reviewed and approved by the University of Georgia Institutional Animal Care and Use Committee (IACUC). Ferrets were anesthetized with a mixture of oxygen and 5% isoflurane for infection and nasal washes.

**Coinfection in naive ferrets and direct contact transmission.** Ferrets ( $n = 40$ ) were randomly divided into 10 groups ( $n = 4$ ). Five groups were directly single-infected with IAV or SARS-CoV-2 or coinfecting with SARS-CoV-2 and IAV intranasally (naive transmitter ferrets) in a 1 mL (500  $\mu$ L instilled in each nostril). Influenza A/California/07/2009 H1N1 ( $10^6$  PFU), influenza A/Kansas/14/2017 H3N2 ( $1.3 \times 10^9$  PFU), and SARS-CoV-2 ( $5 \times 10^5$  PFU) were used for infection. Twenty-four hours postinfection, nasal washes were performed on those transmitter ferrets, and another five groups of naive ferrets ( $n = 4$ ) (receiver ferrets) were cohoused with the naive transmitter ferrets for direct contact transmission. Nasal washes were further collected from naive transmitter ferrets on days 3, 5, 7, and 9 d postinfection (pi) or from receiver ferrets on 2, 4, 6, 8, and 10 d postexposure (pe) to the naive transmitters. All nasal wash samples were then stored at  $-80^\circ\text{C}$  for further use.

**Coinfection in vaccinated ferrets and direct contact transmission.** A separate subset of ferrets ( $n = 30$ ) was randomly divided into 10 groups ( $n = 3$ ). Five groups of ferrets have intramuscularly vaccinated with the 2019 to 2020 Fluzone quadrivalent seasonal influenza vaccine (Sanofi Pasteur, Swiftwater, PA, USA) on days 0 and 28 (250  $\mu$ L/dose). Blood samples were collected from all ferrets on day 0 to make sure they are all seronegative to vaccine components by the hemagglutination inhibition assay. On day 42, blood (3 mL) was collected to assess antibody seroconversion to vaccine strains. On day 56, vaccinated ferrets were single-infected with either IAV or SARS-CoV-2 or coinfecting with those two viruses (vaccinated transmitter ferrets) and nasal washes were collected as described above. All ferrets were monitored daily for up to 14 days during the infection or exposure, and body weights were recorded daily.

**Histopathology evaluation of coinfecting ferrets.** Fifteen ferrets ( $n = 3/\text{group}$ ) were single-infected with IAVs or SARS-CoV-2 or coinfecting with IAV and SARS-CoV-2 simultaneously. At 4 d pi, all infected ferrets were euthanized with B-euthanasia, and lungs were inflated with neutral-buffered 10% formalin. One week later, lung tissue was removed from formalin and then immersed into 70% ethanol until being processed. For the nasal cavity, ferret heads were removed and fixed in neutral buffered 10% formalin and subjected to decalcification in Kristensen's solution. Tissues were subsequently processed, embedded in paraffin, sectioned at 5  $\mu$ m, and stained with hematoxylin and eosin (H&E) as described before (62). Histopathological evaluation of lungs and nasal cavities was performed by a board-certified pathologist. Lesion severity and distribution were evaluated and scored: 0 = no histological change; lesion severity: 1 = minimal, 2 = mild, 3 = moderate, 4 = severe; lesion distribution: 1 = focal, 2 = multifocal, 3 = diffuse.

**Influenza virus titers by plaque assay.** Madine Darby canine kidney (MDCK) cells were seeded at  $5 \times 10^5$  cells per well of a 12-well plate the day before. The cells were inoculated with 100  $\mu$ L of 10-fold serial dilutions of nasal wash samples or lung homogenates (final dilution factors ranging from  $10^8$  to  $10^{-6}$ ) for 1 h with intermittent shaking every 15 min. The cells were washed with PBS after 1 h inoculation and cultured in 2 mL of overlay medium, containing  $1 \times$  MEM supplemented with 10,000 U/mL PEN-STREP, 2 mM L-Glu, 1.5 mg/mL NaHCO<sub>3</sub>, 10 mM HEPES, 5  $\mu$ g/mL Gentamycin, 1.2% Avicel RC-591 NF (MFC corporation, PA, USA), and 1  $\mu$ g/mL trypsin (N-tosyl-L-phenylalanine chloromethyl ketone [TPCK]-treated trypsin; Sigma-Aldrich). Three days after inoculation, the overlay medium was removed. The cells were washed twice with PBS and fixed with 10% buffered formalin, and then stained with 1% crystal violet for 10 min. The plates were then thoroughly washed in distilled water to remove excess crystal violet before being air-dried. The numbers of plaques were counted and the numbers of PFU per milliliter (PFU/mL) were calculated and transformed by  $\log_{10}$ . The limit of detection was 10 PFU/mL nasal wash or  $1 \log_{10}$  (PFU/mL).

**SARS-CoV-2 viral titers by TCID<sub>50</sub>.** Nasal washes or lung homogenates were titrated in quadruplicates in Vero E6 cells. Briefly, confluent VeroE6 cells were inoculated with 2-fold serial dilutions of sample in DMEM containing 2% FBS, supplemented with 1% penicillin-streptomycin (10,000 IU/mL). After 3 days of incubation at 37°C with 5% CO<sub>2</sub>, virus positivity was assessed by reading out cytopathic effects. Infectious virus titers (TCID<sub>50</sub>/mL) were calculated from four replicates of each nasal wash using the Reed–Muench method (63).

**Statistical analysis.** All data were analyzed with Prism 9.0 (GraphPad Software Inc.). One-way analysis of variance (ANOVA) was used to determine the significant differences of virus titers and viral gene copy numbers at different time points within the same infected group. Two-way ANOVA was used to analyze significant differences in body weight, virus titers, and viral gene copy numbers postinfection among different groups.  $P < 0.05$  was considered statistically significant: \*,  $P < 0.05$ ; \*\*,  $P < 0.01$ ; \*\*\*,  $P < 0.001$ ; \*\*\*\*,  $P < 0.0001$ .

## ACKNOWLEDGMENTS

We thank Anne-Gaelle Bebin-Blackwell for their technical assistance. The following reagent was deposited by the Centers for Disease Control and Prevention and obtained through BEI Resources, NIAID, NIH: SARS-Related Coronavirus 2, Isolate USA-WA1/2020, NR-52281.

This project was funded, in part, by the National Institute of Allergy and Infectious Diseases, a component of the NIH, Department of Health and Human Services, under contract 75N93019C00052 and the University of Georgia (UGA) (UGA-001). The content is solely the responsibility of the authors and does not necessarily represent the official views of the NIH. In addition, T.M.R. is supported by the Georgia Research Alliance as an Eminent Scholar.

We declare no conflict of interest.

## REFERENCES

- Li Q, Guan X, Wu P, Wang X, Zhou L, Tong Y, Ren R, Leung KSM, Lau EHY, Wong JY, Xing X, Xiang N, Wu Y, Li C, Chen Q, Li D, Liu T, Zhao J, Liu M, Tu W, Chen C, Jin L, Yang R, Wang Q, Zhou S, Wang R, Liu H, Luo Y, Liu Y, Shao G, Li H, Tao Z, Yang Y, Deng Z, Liu B, Ma Z, Zhang Y, Shi G, Lam TTY, Wu JT, Gao GF, Cowling BJ, Yang B, Leung GM, Feng Z. 2020. Early Transmission Dynamics in Wuhan, China, of Novel Coronavirus-Infected Pneumonia. *N Engl J Med* 382:1199–1207. <https://doi.org/10.1056/NEJMoa2001316>.
- Voss JD, Skarzynski M, McAuley EM, Maier EJ, Gibbons T, Fries AC, Chapleau RR. 2021. Variants in SARS-CoV-2 associated with mild or severe outcome. *Evol Med Public Health* 9:267–275. <https://doi.org/10.1093/emph/eoab019>.
- Science brief: emerging SARS-CoV-2 variants, in CDC COVID-19 Science Briefs. 2020. Atlanta (GA).
- Dong E, Du H, and Gardner L. 2020. An interactive web-based dashboard to track COVID-19 in real time. *Lancet Infect Dis* 20:533–534. [https://doi.org/10.1016/S1473-3099\(20\)30120-1](https://doi.org/10.1016/S1473-3099(20)30120-1).
- CDC. Morbidity and Mortality Weekly Report (MMWR). Center for Disease Control and Prevention, 2021.
- Kirby T. 2021. New variant of SARS-CoV-2 in UK causes surge of COVID-19. *Lancet Respir Med* 9:e20–e21. [https://doi.org/10.1016/S2213-2600\(21\)00005-9](https://doi.org/10.1016/S2213-2600(21)00005-9).
- Washington NL, Gangavarapu K, Zeller M, Bolze A, Cirulli ET, Schiabor Barrett KM, Larsen BB, Anderson C, White S, Cassens T, Jacobs S, Levan G, Nguyen J, Ramirez JM, Rivera-Garcia C, Sandoval E, Wang X, Wong D, Spencer E, Robles-Sikisaka R, Kurzban E, Hughes LD, Deng X, Wang C, Servellita V, Valentine H, De Hoff P, Seaver P, Sathe S, Gietzen K, Sickler B, Antico J, Hoon K, Liu J, Harding A, Bakhtar O, Basler T, Austin B, MacCannell D, Isaksson M, Febbo PG, Becker D, Laurent M, McDonald E, Yeo GW, Knight R, Laurent LC, de Feo E, Worobey M, Chiu CY, et al. 2021. Emergence and rapid transmission of SARS-CoV-2 B.1.1.7 in the United States. *Cell* 184:2587–2594.e7. <https://doi.org/10.1016/j.cell.2021.03.052>.
- Galloway SE, Paul P, MacCannell DR, Johansson MA, Brooks JT, MacNeil A, Slayton RB, Tong S, Silk BJ, Armstrong GL, Biggerstaff M, Dugan VG. 2021. Emergence of SARS-CoV-2 B.1.1.7 Lineage - United States, December 29, 2020-January 12, 2021. *MMWR Morb Mortal Wkly Rep* 70:95–99. <https://doi.org/10.15585/mmwr.mm7003e2>.
- Kiefer MK, Allen KD, Russo JR, Ma'ayah M, Gee SE, Kniss D, Cackovic M, Costantine MM, Rood KM. 2021. Decline in Sars-CoV-2 antibodies over 6-month follow-up in obstetrical healthcare workers. *Am J Reprod Immunol* 86:e13490. <https://doi.org/10.1111/aji.13490>.
- Cavanaugh AM, Spicer KB, Thoroughman D, Glick C, Winter K. 2021. Reduced risk of reinfection with SARS-CoV-2 after COVID-19 vaccination - Kentucky, May-June 2021. *MMWR Morb Mortal Wkly Rep* 70:1081–1083. <https://doi.org/10.15585/mmwr.mm7032e1>.
- Garduno-Orbe B, et al. 2021. SARS-CoV-2 Reinfection among healthcare workers in Mexico: case report and literature review. *Medicina (Kaunas)* 57:442. <https://doi.org/10.3390/medicina57050442>.
- Olsen SJ, Azziz-Baumgartner E, Budd AP, Brammer L, Sullivan S, Pineda RF, Cohen C, Fry AM. 2020. Decreased influenza activity during the COVID-19 pandemic - United States, Australia, Chile, and South Africa, 2020. *MMWR Morb Mortal Wkly Rep* 69:1305–1309. <https://doi.org/10.15585/mmwr.mm6937a6>.
- Renn M, Bartok E, Zillinger T, Hartmann G, Behrendt R. 2021. Animal models of SARS-CoV-2 and COVID-19 for the development of prophylactic and therapeutic interventions. *Pharmacol Ther* 228:107931. <https://doi.org/10.1016/j.pharmthera.2021.107931>.
- Alberca RW. 2021. Animal models and COVID-19: mechanism and comorbidities. *Respirology* 26:616–617. <https://doi.org/10.1111/resp.14043>.
- Hodgson J. 2020. The pandemic pipeline. *Nat Biotechnol* 38:523–532. <https://doi.org/10.1038/d41587-020-00005-z>.
- Kumar S, Yadav PK, Srinivasan R, Perumal N. 2020. Selection of animal models for COVID-19 research. *VirusDis* 31:453–456. <https://doi.org/10.1007/s13337-020-00637-4>.
- Winkler ES, Gilchuk P, Yu J, Bailey AL, Chen RE, Chong Z, Zost SJ, Jang H, Huang Y, Allen JD, Case JB, Sutton RE, Carnahan RH, Darling TL, Boon ACM, Mack M, Head RD, Ross TM, Crowe JE, Diamond MS. 2021. Human neutralizing antibodies against SARS-CoV-2 require intact Fc effector functions for optimal therapeutic protection. *Cell* 184:1804–1820.e16. <https://doi.org/10.1016/j.cell.2021.02.026>.
- McCray PB, Pewe L, Wohlford-Lenane C, Hickey M, Manzel L, Shi L, Netland J, Jia HP, Halabi C, Sigmund CD, Meyerholz DK, Kirby P, Look DC, Perlman S. Jr. 2007. Lethal infection of K18-hACE2 mice infected with severe acute respiratory syndrome coronavirus. *J Virol* 81:813–821. <https://doi.org/10.1128/JVI.02012-06>.
- Tseng C-TK, Huang C, Newman P, Wang N, Narayanan K, Watts DM, Makino S, Packard MM, Zaki SR, Chan T-S, Peters CJ. 2007. Severe acute respiratory syndrome coronavirus infection of mice transgenic for the human Angiotensin-converting enzyme 2 virus receptor. *J Virol* 81:1162–1173. <https://doi.org/10.1128/JVI.01702-06>.
- Rathnasinghe R, Strohmeier S, Amanat F, Gillespie VL, Krammer F, Garcia-Sastre A, Coughlan L, Schotsaert M, Uccellini MB. 2020. Comparison of transgenic and adenovirus hACE2 mouse models for SARS-

- CoV-2 infection. *Emerg Microbes Infect* 9:2433–2445. <https://doi.org/10.1080/22221751.2020.1838955>.
21. Munoz-Fontela C, et al. 2020. Animal models for COVID-19. *Nature* 586: 509–515. <https://doi.org/10.1038/s41586-020-2787-6>.
  22. Sia SF, Yan L-M, Chin AWH, Fung K, Choy K-T, Wong AYL, Kaewpreedee P, Perera RAPM, Poon LLM, Nicholls JM, Peiris M, Yen H-L. 2020. Pathogenesis and transmission of SARS-CoV-2 in golden hamsters. *Nature* 583: 834–838. <https://doi.org/10.1038/s41586-020-2342-5>.
  23. Chan JF, et al. 2020. Simulation of the clinical and pathological manifestations of coronavirus disease 2019 (COVID-19) in a golden syrian hamster model: implications for disease pathogenesis and transmissibility. *Clin Infect Dis* 71:2428–2446. <https://doi.org/10.1093/cid/ciaa325>.
  24. Zhang AJ, Lee AC-Y, Chan JF-W, Liu F, Li C, Chen Y, Chu H, Lau S-Y, Wang P, Chan CC-S, Poon VK-M, Yuan S, To KK-W, Chen H, Yuen K-Y. 2021. Coinfection by severe acute respiratory syndrome coronavirus 2 and influenza A(H1N1)pdm09 virus enhances the severity of pneumonia in golden syrian hamsters. *Clin Infect Dis* 72:e978–e992. <https://doi.org/10.1093/cid/ciaa1747>.
  25. Enkirsch T, and, von Messling V. 2015. Ferret models of viral pathogenesis. *Virology* 479–480:259–270. <https://doi.org/10.1016/j.virol.2015.03.017>.
  26. Kim Y-I, Kim S-G, Kim S-M, Kim E-H, Park S-J, Yu K-M, Chang J-H, Kim EJ, Lee S, Casel MAB, Um J, Song M-S, Jeong HW, Lai VD, Kim Y, Chin BS, Park J-S, Chung K-H, Foo S-S, Poo H, Mo I-P, Lee O-J, Webby RJ, Jung JU, Choi YK. 2020. Infection and rapid transmission of SARS-CoV-2 in ferrets. *Cell Host Microbe* 27:704–709.e2. <https://doi.org/10.1016/j.chom.2020.03.023>.
  27. Schlottau K, Rissmann M, Graaf A, Schön J, Sehl J, Wylezich C, Höper D, Mettenleiter TC, Balkema-Buschmann A, Harder T, Grund C, Hoffmann D, Breithaupt A, Beer M. 2020. SARS-CoV-2 in fruit bats, ferrets, pigs, and chickens: an experimental transmission study. *Lancet Microbe* 1: e218–e225. [https://doi.org/10.1016/S2666-5247\(20\)30089-6](https://doi.org/10.1016/S2666-5247(20)30089-6).
  28. Shi J, Wen Z, Zhong G, Yang H, Wang C, Huang B, Liu R, He X, Shuai L, Sun Z, Zhao Y, Liu P, Liang L, Cui P, Wang J, Zhang X, Guan Y, Tan W, Wu G, Chen H, Bu Z. 2020. Susceptibility of ferrets, cats, dogs, and other domesticated animals to SARS-coronavirus 2. *Science* 368:1016–1020. <https://doi.org/10.1126/science.abb7015>.
  29. Huang C, Wang Y, Li X, Ren L, Zhao J, Hu Y, Zhang L, Fan G, Xu J, Gu X, Cheng Z, Yu T, Xia J, Wei Y, Wu W, Xie X, Yin W, Li H, Liu M, Xiao Y, Gao H, Guo L, Xie J, Wang G, Jiang R, Gao Z, Jin Q, Wang J, Cao B. 2020. Clinical features of patients infected with 2019 novel coronavirus in Wuhan, China. *Lancet* 395: 497–506. [https://doi.org/10.1016/S0140-6736\(20\)30183-5](https://doi.org/10.1016/S0140-6736(20)30183-5).
  30. Cascella M, et al. Features, Evaluation, and Treatment of Coronavirus (COVID-19), in StatPearls. 2021. Treasure Island (FL).
  31. van Riel D, Munster VJ, de Wit E, Rimmelzwaan GF, Fouchier RAM, Osterhaus ADME, Kuiken T. 2007. Human and avian influenza viruses target different cells in the lower respiratory tract of humans and other mammals. *Am J Pathol* 171:1215–1223. <https://doi.org/10.2353/ajpath.2007.070248>.
  32. Liu J, Li Y, Liu Q, Yao Q, Wang X, Zhang H, Chen R, Ren L, Min J, Deng F, Yan B, Liu L, Hu Z, Wang M, Zhou Y. 2021. SARS-CoV-2 cell tropism and multiorgan infection. *Cell Discov* 7:17. <https://doi.org/10.1038/s41421-021-00249-2>.
  33. Murphy K. 2020. SARS CoV-2 detection from upper and lower respiratory tract specimens: diagnostic and infection control implications. *Chest* 158: 1804–1805. <https://doi.org/10.1016/j.chest.2020.07.061>.
  34. Scialo F, Daniele A, Amato F, Pastore L, Matera MG, Cazzola M, Castaldo G, Bianco A. 2020. ACE2: the major cell entry receptor for SARS-CoV-2. *Lung* 198:867–877. <https://doi.org/10.1007/s00408-020-00408-4>.
  35. Luo M. 2012. Influenza virus entry. *Adv Exp Med Biol* 726:201–221. [https://doi.org/10.1007/978-1-4614-0980-9\\_9](https://doi.org/10.1007/978-1-4614-0980-9_9).
  36. Yue H, Zhang M, Xing L, Wang K, Rao X, Liu H, Tian J, Zhou P, Deng Y, Shang J. 2020. The epidemiology and clinical characteristics of co-infection of SARS-CoV-2 and influenza viruses in patients during COVID-19 outbreak. *J Med Virol* 92:2870–2873. <https://doi.org/10.1002/jmv.26163>.
  37. Stowe J, Tessier L, Zhao H, Guy R, Muller-Pebody B, Zambon M, Andrews N, Ramsay M, Lopez BJ. Interactions between SARS-CoV-2 and influenza and the impact of coinfection on disease severity: a test negative design. *Int J Epi* 50:1124–1133. <https://doi.org/10.1093/ije/dyab081>.
  38. Carter DM, Bloom CE, Nascimento EJM, Marques ETA, Craigio JK, Cherry JL, Lipman DJ, Ross TM. 2013. Sequential seasonal H1N1 influenza virus infections protect ferrets against novel 2009 H1N1 influenza virus. *J Virol* 87:1400–1410. <https://doi.org/10.1128/JVI.02257-12>.
  39. World Health Organization. [https://www.who.int/news-room/fact-sheets/detail/influenza-\(seasonal\)](https://www.who.int/news-room/fact-sheets/detail/influenza-(seasonal)). 2018. November.
  40. Thompson WW, Shay DK, Weintraub E, Brammer L, Cox N, Anderson LJ, Fukuda K. 2003. Mortality associated with influenza and respiratory syncytial virus in the United States. *JAMA* 289:179–186. <https://doi.org/10.1001/jama.289.2.179>.
  41. Putri WCWS, Muscatello DJ, Stockwell MS, Newall AT. 2018. Economic burden of seasonal influenza in the United States. *Vaccine* 36:3960–3966. <https://doi.org/10.1016/j.vaccine.2018.05.057>.
  42. Singh B, Kaur P, Reid R-J, Shamoon F, Bikkina M. 2020. COVID-19 and influenza co-infection: report of three cases. *Cureus* 12:e9852. <https://doi.org/10.7759/cureus.9852>.
  43. Ozaras R, Cirpin R, Duran A, Duman H, Arslan O, Bakcan Y, Kaya M, Mutlu H, Isayeva L, Kebanli F, Deger BA, Bekeshev E, Kaya F, Bilir S. 2020. Influenza and COVID-19 coinfection: report of six cases and review of the literature. *J Med Virol* 92:2657–2665. <https://doi.org/10.1002/jmv.26125>.
  44. Munivenkatappa A, Yadav PD, Swetha K, Jayaswamy M, Nyayanit DA, Sahay R, Basavaraj TJ. 2021. SARS-CoV-2 & influenza A virus co-infection in an elderly patient with pneumonia. *Indian J Med Res* 153:190. [https://doi.org/10.4103/ijmr.IJMR\\_2711\\_20](https://doi.org/10.4103/ijmr.IJMR_2711_20).
  45. Cuadrado-Payan E, et al. 2020. SARS-CoV-2 and influenza virus co-infection. *Lancet* 395:e84. [https://doi.org/10.1016/S0140-6736\(20\)31052-7](https://doi.org/10.1016/S0140-6736(20)31052-7).
  46. Wu X, Cai Y, Huang X, Yu X, Zhao L, Wang F, Li Q, Gu S, Xu T, Li Y, Lu B, Zhan Q. 2020. Co-infection with SARS-CoV-2 and influenza A virus in patient with pneumonia, China. *Emerg Infect Dis* 26:1324–1326. <https://doi.org/10.3201/eid2606.200299>.
  47. Zheng X, Wang H, Su Z, Li W, Yang D, Deng F, Chen J. 2020. Co-infection of SARS-CoV-2 and influenza virus in early stage of the COVID-19 epidemic in Wuhan, China. *J Infect* 81:e128–e129. <https://doi.org/10.1016/j.jinf.2020.05.041>.
  48. Ding Q, Lu P, Fan Y, Xia Y, Liu M. 2020. The clinical characteristics of pneumonia patients coinfecting with 2019 novel coronavirus and influenza virus in Wuhan, China. *J Med Virol* 92:1549–1555. <https://doi.org/10.1002/jmv.25781>.
  49. Hashemi SA, Safamanesh S, Ghasemzadeh-Moghaddam H, Ghafouri M, Azimian A. 2021. High prevalence of SARS-CoV-2 and influenza A virus (H1N1) coinfection in dead patients in Northeastern Iran. *J Med Virol* 93: 1008–1012. <https://doi.org/10.1002/jmv.26364>.
  50. Bai L, Zhao Y, Dong J, Liang S, Guo M, Liu X, Wang X, Huang Z, Sun X, Zhang Z, Dong L, Liu Q, Zheng Y, Niu D, Xiang M, Song K, Ye J, Zheng W, Tang Z, Tang M, Zhou Y, Shen C, Dai M, Zhou L, Chen Y, Yan H, Lan K, Xu K. 2021. Coinfection with influenza A virus enhances SARS-CoV-2 infectivity. *Cell Res* 31:395–403. <https://doi.org/10.1038/s41422-021-00473-1>.
  51. Achdout H, Vitner EB, Politi B, Melamed S, Yahalom-Ronen Y, Tamir H, Erez N, Avraham R, Weiss S, Cherry L, Bar-Haim E, Makdasi E, Gur D, Aftalion M, Chitlaru T, Vagima Y, Paran N, Israely T. 2021. Increased lethality in influenza and SARS-CoV-2 coinfection is prevented by influenza immunity but not SARS-CoV-2 immunity. *Nat Commun* 12:5819. <https://doi.org/10.1038/s41467-021-26113-1>.
  52. Bao L, et al. 2021. Sequential infection with H1N1 and SARS-CoV-2 aggravated COVID-19 pathogenesis in a mammalian model, and co-vaccination as an effective method of prevention of COVID-19 and influenza. *Signal Transduct Target Ther* 6:200. <https://doi.org/10.1038/s41392-021-00618-z>.
  53. Ryan KA, Bewley KR, Fotheringham SA, Slack GS, Brown P, Hall Y, Wand NI, Marriott AC, Cavell BE, Tree JA, Allen L, Aram MJ, Bean TJ, Brunt E, Buttigieg KR, Carter DP, Cobb R, Coombes NS, Findlay-Wilson SJ, Godwin KJ, Gooch KE, Gouriet J, Halkerston R, Harris DJ, Hender TH, Humphries HE, Hunter L, Ho CMK, Kennard CL, Leung S, Longet S, Ngabo D, Osman KL, Paterson J, Penn EJ, Pullan ST, Rayner E, Skinner O, Steeds K, Taylor I, Tipton T, Thomas S, Turner C, Watson RJ, Wiblin NR, Charlton S, Hallis B, Hiscox JA, Funnell S, Dennis MJ, et al. 2021. Dose-dependent response to infection with SARS-CoV-2 in the ferret model and evidence of protective immunity. *Nat Commun* 12:81. <https://doi.org/10.1038/s41467-020-20439-y>.
  54. Patel DR, Field CJ, Septer KM, Sim DG, Jones MJ, Heinly TA, Vanderford TH, McGraw EA, Sutton TC. 2021. Transmission and Protection against Reinfection in the Ferret Model with the SARS-CoV-2 USA-WA1/2020 Reference Isolate. *J Virol* 95:e0223220. <https://doi.org/10.1128/JVI.02232-20>.
  55. Bodewes R, Kreijtz JHCM, van Amerongen G, Hillaire MLB, Vogelzang-van Trierum SE, Nieuwkoop NJ, van Run P, Kuiken T, Fouchier RAM, Osterhaus ADME, Rimmelzwaan GF. 2013. Infection of the upper respiratory tract with seasonal influenza A(H3N2) virus induces protective immunity in ferrets against infection with A(H1N1)pdm09 virus after intranasal, but not intratracheal, inoculation. *J Virol* 87:4293–4301. <https://doi.org/10.1128/JVI.02536-12>.
  56. Rossman JS, and, Lamb RA. 2011. Influenza virus assembly and budding. *Virology* 411:229–236. <https://doi.org/10.1016/j.virol.2010.12.003>.
  57. Shinya K, and, Kawakami Y. 2006. [Influenza virus receptors in the human airway]. *Uirus* 56:85–89. <https://doi.org/10.2222/jsv.56.85>.

58. Shinya K, Ebina M, Yamada S, Ono M, Kasai N, Kawaoka Y. 2006. Avian flu: influenza virus receptors in the human airway. *Nature* 440:435–436. <https://doi.org/10.1038/440435a>.
59. Pinky L, and, Dobrovoly HM. 2016. Coinfections of the Respiratory Tract: viral Competition for Resources. *PLoS One* 11:e0155589. <https://doi.org/10.1371/journal.pone.0155589>.
60. Nickbakhsh S, et al. 2019. Virus-virus interactions impact the population dynamics of influenza and the common cold. *Proc Natl Acad Sci U S A* 116:27142–27150. <https://doi.org/10.1073/pnas.1911083116>.
61. Richard M, Kok A, de Meulder D, Bestebroer TM, Lamers MM, Okba NMA, Fentener van Vlissingen M, Rockx B, Haagmans BL, Koopmans MPG, Fouchier RAM, Herfst S. 2020. SARS-CoV-2 is transmitted via contact and via the air between ferrets. *Nat Commun* 11:3496. <https://doi.org/10.1038/s41467-020-17367-2>.
62. Huang Y, França MS, Allen JD, Shi H, Ross TM. 2021. Next Generation of computationally optimized broadly reactive ha vaccines elicited cross-reactive immune responses and provided protection against H1N1 virus infection. *Vaccines (Basel)* 9:793. <https://doi.org/10.3390/vaccines9070793>.
63. Ramakrishnan MA. 2016. Determination of 50% endpoint titer using a simple formula. *World J Virol* 5:85–86. <https://doi.org/10.5501/wjv.v5.i2.85>.